[9] M. Saunders, J. B. Hyne, *J. Chem. Phys.* **1958**, *29*, 1319.
[10] This crystal structure was solved based on the two zinc(II) porphyrin molecules, and the tetrameric form was obtained by its expansion. This crystal also contains fourteen disordered benzene molecules per tetraporphyrin which fill large empty spaces. Crystal data for **Z1**: $C_{78}H_{70}Zn_2N_{10}\cdot 7\,C_6H_6$, $M_r = 1825$, crystal from C_6H_6/CH_3CN, crystal dimensions $0.35 \times 0.2 \times 0.2$ mm, space group monoclinic ($P2_1/n$), $a = 13.7485(2)$, $b = 18.3200(3)$, $c = 40.8739(7)$ Å, $\alpha = 90$, $\beta = 84.1947(3)$, $\gamma = 90°$, $V = 10\,242.2(2)$ Å^3, $Z = 8$, $\rho_{calcd} = 2.367$ g cm^{-3}; $\mu_{Mo} = 10.44$ cm^{-1}; $\theta_{max} = 27.3°$. For 63 126 reflections measured; $R_1 = 0.099$ for 9459 data [$I > 3\sigma(I)$], $wR_2 = 0.143$ for all measured data. The structures of all the compounds were solved by direct methods and refined by F^2 with all observed reflections. All non-hydrogen atoms without disordered *tert*-butyl group and incorporated solvent molecules were refined anisotropically, and hydrogen atoms were added to calculated positions. Programs used were structure determination by SIR92 and refinement by teXane for Windows. CCDC-173782 (**Z1**)$_4$ contains the supplementary crystallographic data for this paper. These data can be obtained free of charge via www.ccdc.cam.ac.uk/conts/retrieving.html (or from the Cambridge Crystallographic Data Centre, 12, Union Road, Cambridge CB2 1EZ, UK; fax: (+44) 1223-336-033; or deposit@ccdc.cam.ac.uk).
[11] A. Nakano, H. Shimidzu, A. Osuka, *Tetrahedron Lett.* **1998**, *39*, 9489.
[12] a) Y. Deng, C. K. Chang, D. G. Nocera, *Angew. Chem.* **2000**, *112*, 1108; *Angew. Chem. Int. Ed.* **2000**, *39*, 1066; b) N. Aratani, A. Osuka, *Org. Lett.* **2001**, *3*, 4213.
[13] S. Sakamoto, M. Fujita, K. Kim, K. Yamaguchi, *Tetrahedron* **2000**, *56*, 955. CSI-MS spectrum measurement was performed with sector mass spectrometer (JMS-700, JEOL) equipped with the CSI source. Typical measurement conditions are as follows: (CSI-MS) acceleration voltage, 3.0 kV; needle voltage, 2.9 kV; orifice voltage, 197 V; resolution (10% valley definition), 1000; sample flow, 17 μL min^{-1}; solvent, dry THF; concentration, 10 mmol L^{-1}; spray temperature, 4 °C; ion-source temperature, 15 °C.
[14] This consideration in turn suggests that apparently stronger electronic interactions in the normal *meso*–*meso*-linked diporphyrins result from the rotational flexibility around the *meso*–*meso* single bond.
[15] Selected ^{1}H NMR signals of the pyridyl groups of (**Z2**)$_4$ in [D$_8$]THF; $\delta = 2.62$, 3.11, 6.59, and 6.86 ppm.
[16] N. Yoshida, A. Osuka, *Tetrahedron Lett.* **2000**, *41*, 9287.

Crystal Engineering of a Nanoscale Kagomé Lattice**

Brian Moulton, Jianjiang Lu, Ranko Hajndl, Srikanth Hariharan, and Michael J. Zaworotko*

What would the properties of materials be if we could really arrange the atoms the way we want them? Although this question is scientifically and technologically topical, it is a well-known excerpt from the Richard P. Feynman lecture "There's Plenty of Room at the Bottom".[1] Recent advances in our understanding of supramolecular chemistry offer promise that Feynman's dream will be realized since they have afforded design principles that have provided access to an array of new solid phases with specific and, in many cases, previously unknown molecular topologies. Indeed, as molecular scientists become ever more proficient at the supramolecular synthesis[2] of new compositions and structures, the question that might now be posed is: "in what manner do we want to arrange the atoms?" In the context of magnetic materials, theorists have provided chemists with an array of target lattices,[3] and synthetic chemists have developed new strategies for the generation of novel networks that contain magnetic components.[4–7] Spin-frustrated lattices represent attractive targets that are exemplified by the antiferromagnetic Kagomé lattice.[8] Herein we present the synthesis, crystal structure, and magnetic properties of, what is to our knowledge, the first example of a nanoscale Kagomé lattice.

The phase is sustained by paramagnetic dicopper(II) tetracarboxylate spin pairs (metal dimers) positioned at the vertices of a Kagomé lattice, and it exploits the concept of self-assembly of nanoscale secondary building units (nSBUs).[9] It therefore offers a system where the effect of systematically substituting the molecular components can be evaluated. In this context, we compare the magnetic response of the Kagomé lattice arrangement with a system where identical secondary building units (SBUs)[10] are arranged in a tetragonal 2D configuration, which is not expected to exhibit spin frustration.

We have recently demonstrated that regular molecular squares can self-assemble at their vertices to form square or triangular nSBUs, and that the use of an appropriate template and mild crystallization conditions facilitates the generation of a diverse range of discrete and infinite molecular architectures that are based upon these nSBUs.[9, 11–13] The ubiquitous dimetal tetracarboxylates [$M_2L_2(O_2CR)_4$] (L = coordinated ligand, M = transition metal) serve as ideal molecular squares in this context since they are synthetically accessible and, depending upon the metal, offer potential as catalysts[14] or molecular magnets.[15, 16] Figure 1 illustrates the two nSBUs that can be generated if the molecular squares are linked by 1,3-benzenedicarboxylate (bdc), that is, at 120°: a square nSBU (a cluster of four square SBUs) or a triangular nSBU (a cluster of three square SBUs). These nSBUs are known to self-assemble to form discrete nanoballs (sustained by both square and triangular nSBUs)[12] or a tetragonal 2D lattice (sustained by square nSBUs only).[9] It occurred to us that other supramolecular isomers are possible if triangular nSBUs alone are present: triangular or Kagomé 2D lattices (Figure 2). Few examples of molecular Kagomé lattices have been reported to date,[17–19] and to our knowledge there have been no reports of a nanoscale lattice, despite the expectation of cooperative magnetic phenomena in such structures.

Slow diffusion of ethanolic copper(II) nitrate into a solution of bdc, pyridine (py), and an appropriate template (nitrobenzene, 1,2-dichlorobenzene, or naphthalene) in ethanol affords prismatic blue-green crystals of [$(Cu_2(py)_2(bdc)_2)_3$]$_n$ (**1**). The crystal structure of **1**[20] (Figure 3) can be described as

[*] Prof. Dr. M. J. Zaworotko, B. Moulton, J. Lu
Department of Chemistry
University of South Florida
4202 E. Fowler Ave., SCA 400, Tampa, FL 33620 (USA)
Fax: (+1) 813-974-1733
E-mail: xtal@usf.edu
R. Hajndl, Prof. Dr. S. Hariharan
Department of Physics
University of South Florida
4202 E. Fowler Ave., PHY 114, Tampa, FL 33620 (USA)

[**] M.J.Z. gratefully acknowledges the financial support of the National Science Foundation (DMR-0101641). S.H. acknowledges support from a DARPA/AMRI subcontract (Grant No. MDA 972-97-1-0003).

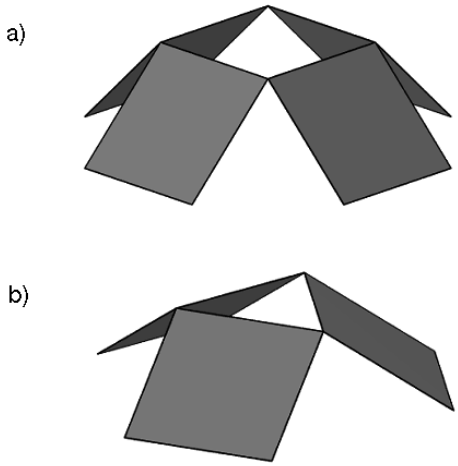

Figure 1. Illustrations of the square (a) and triangular (b) nSBUs that can be formed by linking the vertices of molecular squares.

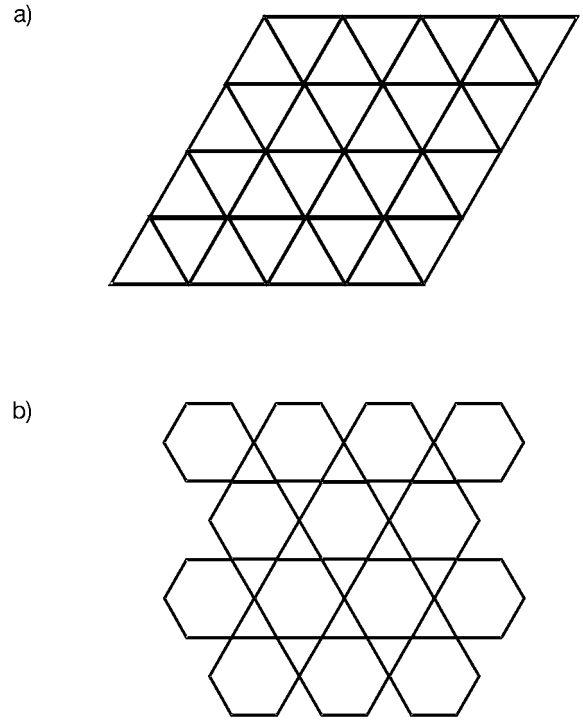

Figure 2. A schematic representation of triangular (a) and Kagomé (b) 2D lattices.

the result of self-assembly of bowl-shaped triangular nSBUs to yield a nanoscale Kagomé lattice. Cu_2 dimers are positioned at the lattice points and are bridged by the bdc ligands, thereby generating large hexagonal cavities within the layer. The bowl-shaped nSBU facilitates efficient packing when the bowls are eclipsed, which results in eclipsing of the hexagonal cavities (0.91 nm effective diameter) and in hexagonal channels of the same dimension. The layers are undulating because of the curvature imparted by the bdc moiety, and have an amplitude of 1.24 nm, with adjacent layers overlapping by approximately 20%. The apical positions of the Cu_2 dimers are occupied by coordinated pyridine ligands, and highly disordered solvent molecules occupy the hexagonal channels (approximately 28% by weight). Thermal analyses

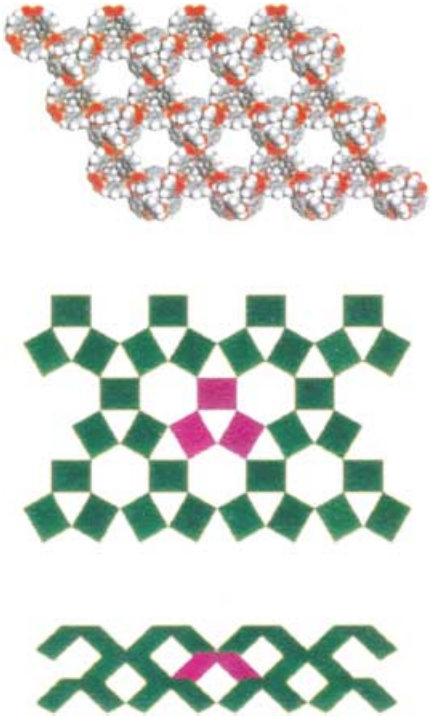

Figure 3. Space-filling and schematic representations of the arrangement of triangular nSBUs in the nanoscale Kagomé lattice structure exhibited by **1**.

(thermogravimetric analysis and differential scanning calorimetry) indicate that the solvent of crystallization and the pyridine ligands can be removed at approximately 200 °C, and that the desolvated lattice is thermally stable at temperatures in excess of 300 °C. The most intense peaks observed in the X-ray powder diffraction patterns from the bulk sample are consistent with those calculated from single-crystal diffraction data. A phase based on square nSBUs, $[((py)_2Cu_2(bdc)_2)_4]_n$ (**2**), can be obtained under different crystallization conditions.[9]

The magnetic properties of **1** are featured in Figure 4. The temperature-dependent susceptibility (χ) at a constant field ($H = 0.1$ T) is shown in Figure 4a and the field-dependent magnetization at low temperature ($T = 5$ K) in Figure 4b. The graphs exhibit rich structure that can be associated with the combined intradimer and interdimer magnetic interactions. Cooperative magnetism in complexes based on Cu_2 dimers has been studied in the past and is known to predominantly exhibit antiferromagnetic coupling.[21, 22]

The temperature-dependent χ shows a maximum just below 300 K and a minimum at around 60 K followed by an upturn at lower temperature. The data presented have been corrected for the diamagnetic contribution. The variation of χ with temperature is consistent with cooperative magnetic behavior observed in dimeric copper complexes. We have used a standard Bleaney–Bowers (BB) model[23] to generate a fit to our experimental data, and this is also shown in Figure 4. The two main fit parameters are the intradimer (J) and interdimer (J') interaction terms. From our fit, we obtain values of $J = -350$ and $J' = -18$ cm^{-1}. Our model also accounts for the presence of uncompensated moments that follow a Curie law.

  1433-7851/02/4115-2822 $ 20.00+.50/0

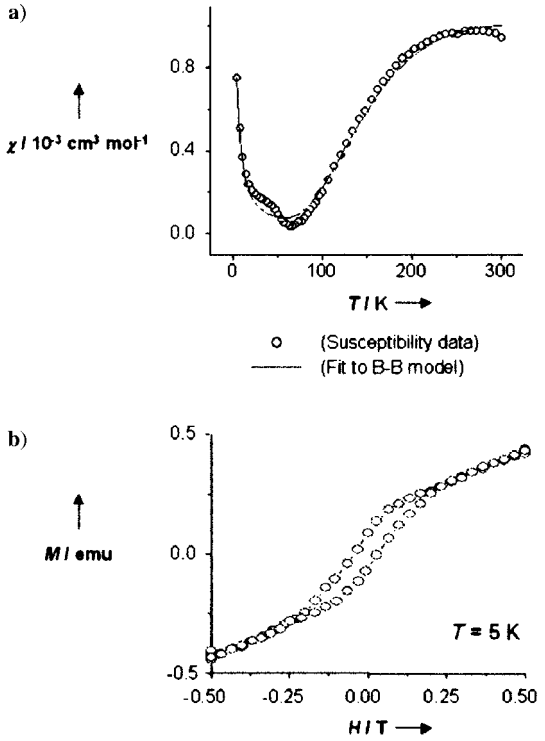

Figure 4. a) The temperature-dependent molar susceptibility (χ, per nSBU) of **1** at 0.1 T (data points) overlaid by a plot of the BB best-fit model (solid line): $J = -350$ cm^{-1} and $J' = -18$ cm^{-1}; b) the field-dependent magnetization of **1** at $T = 5$ K.

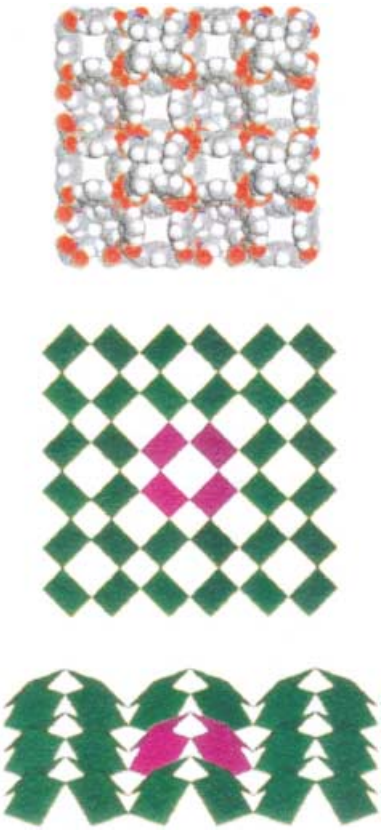

Figure 5. Space-filling and schematic representations of the arrangement of square nSBUs in the nanoscale square lattice structure exhibited by **2**.

This phenomenon is responsible for the upturn in susceptibility at temperatures below 50 K.

A clue as to the nature of the geometrically frustrated antiferromagnetic state inherent in this compound is revealed on investigation of the field-dependent magnetization data, shown in Figure 4b. A well-defined hysteresis loop is observed which is indicative of ferromagnetic behavior. We have also confirmed the presence of hysteresis at 300 K. In a sense, we have demonstrated herein that it is possible to arrange nanoscale molecular objects (not atoms!) with precise control and achieve periodic magnetic nanostructures.[24]

Within the context of the triangular Kagomé lattice, we can now attempt to understand the origin of the ferromagnetic-like response leading to magnetic hysteresis. The triangular lattice framework will result in disruption of perfect antiferromagnetic ordering by introducing spin frustration that leads to canted arrangement of spins. Of course, the term "spins" refers here to the moments of the individual dimers. Spin canting can lead to the appearance of effective weak ferromagnetic long-range order. It has also been pointed out that in low-dimensional systems such as semiconductor quantum dots and molecular magnets, electron correlation effects in an antiferromagnetic lattice can lead to flat-band ferromagnetism.[25]

Phase **2** exhibits an alternative topology to **1**; the 2D square lattice that is shown in Figure 5. In this case, geometry considerations dictate that spin frustration is ruled out, which is reflected in the magnetic measurements shown in Figure 6. To keep our comparison direct and simple, we have plotted molar susceptibility and magnetization data using identical

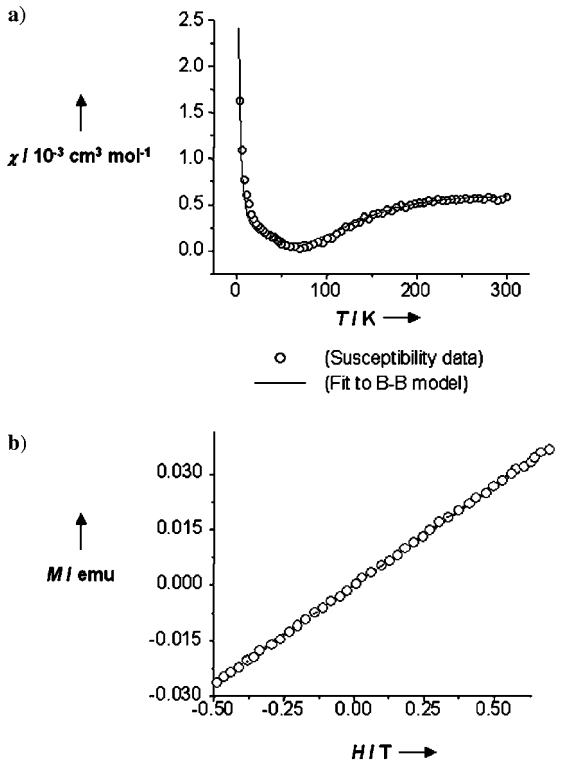

Figure 6. a) The temperature-dependent molar susceptibility (χ, per nSBU) of **2** at 0.1 T (data points) overlaid by a plot of the BB best-fit model (solid line): $J = -380$ cm^{-1} and $J' = -85$ cm^{-1}; b) the field-dependent magnetization of **2** at $T = 5$ K.

  1433-7851/02/4115-2823 $ 20.00+.50/0

conditions to those described in Figure 4. These magnetic data are very similar to recent experimental results reported by other groups on complexes of Cu_2 dimers.[26] Theoretical fit using the BB model to the temperature-dependent molar susceptibility data in this case yields fit parameters $J = -380\ cm^{-1}$ and $J' = -85\ cm^{-1}$. Clearly, the most striking feature is that the field-dependent magnetization does not display a hysteresis loop in this system, the straight line obtained being representative of a more traditional paramagnetic behavior.

Our results dramatically underscore the potential afforded by supramolecular chemistry for the design of molecular nanostructured assemblies with desirable physical properties, while emphasizing how the composition of a material is not the only feature one must consider when designing a phase that exhibits molecular magnetism. Future work will focus on the modularity of this system and on chemical modification of the components: substituting the metal; changing the coordinated ligand; substituting the bdc ligand; incorporation of different guest molecules. We expect a significant effect on magnetic properties as it has already been shown that simply varying the apical coordinated ligand has a measurable effect on the magnetism exhibited by the SBU used in our study.[26]

Received: February 7, 2002 [Z18665]

[1] R. Feynman, *Eng. Sci.* **1960**, 22 – 36.
[2] B. Moulton, M. J. Zaworotko, *Chem. Rev.* **2001**, *101*, 1629 – 1658.
[3] E. Manousakis, *Rev. Mod. Phys.* **1991**, *63*, 1 – 62.
[4] K. R. Dunbar, *J. Solid State Chem.* **2001**, *159*, 251 – 252.
[5] E. Coronado, J. R. Galan-Mascaros, C. J. Gomez-Garcia, V. Laukhin, *Nature* **2000**, *408*, 447 – 449.
[6] S. R. Batten, B. F. Hoskins, B. Moubaraki, K. S. Murray, R. Robson, *Dalton Trans.* **1999**, 2977 – 2986.
[7] S. S. Y. Chui, S. M. F. Lo, J. P. H. Charmant, A. G. Orpen, I. D. Williams, *Science* **1999**, *283*, 1148 – 1150.
[8] I. Syozi, *Prog. Theor. Phys.* **1951**, *6*, 306 – 308.
[9] S. A. Bourne, J. Lu, A. Mondal, B. Moulton, M. J. Zaworotko, *Angew. Chem.* **2001**, *113*, 2111 – 2113; *Angew. Chem. Int. Ed.* **2001**, *40*, 2169 – 2171.
[10] D. W. Breck, *Zeolite Molecular Sieves: Structure, Chemistry and Use*, Wiley-Interscience, New York, **1974**.
[11] J. Lu, A. Mondal, B. Moulton, M. J. Zaworotko, *Angew. Chem.* **2001**, *113*, 2171 – 2174; *Angew. Chem. Int. Ed.* **2001**, *40*, 2113 – 2116.
[12] B. Moulton, J. Lu, A. Mondal, M. J. Zaworotko, *Chem. Commun.* **2001**, 863 – 864.
[13] H. Abourahma, A. W. Coleman, B. Moulton, B. Rather, P. Shahgaldian, M. J. Zaworotko, *Chem. Commun.* **2001**, 2380 – 2381.
[14] D. E. Bergbreiter, M. Morvant, B. Chen, *Tetrahedron Lett.* **1991**, *32*, 2731 – 2734.
[15] O. Kahn, *Molecular Magnetism*, VCH, Weinheim, Germany, **1993**.
[16] J. S. Miller, A. J. Epstein, *MRS Bull.* **2000**, *25*, 21 – 28.
[17] K. Awaga, T. Okuno, A. Yamaguchi, M. Hasegawa, T. Inabe, Y. Maruyama, N. Wada, *Phys. Rev. B* **1994**, *49*, 3975 – 3981.
[18] A. P. Ramirez, *J. Appl. Phys.* **1991**, *70*, 5952 – 5955.
[19] M. G. Townsend, G. Longworth, E. Roudaut, *Phys. Rev. B* **1986**, *33*, 4919 – 4926.
[20] Intensity data for **1** were collected at 173 K on a Bruker SMART-APEX diffractometer using $Mo_{K\alpha}$ radiation ($\lambda = 0.7107$ Å): $Cu_6C_{123.08}H_{54}N_{9.37}O_{30.73}$, 2536.69 g mol^{-1}, trigonal, space group $P\bar{3}c1$, $a = b = 18.6523(11)$, $c = 19.8313(18)$ Å, $V = 5975.1(7)$ Å^3, $Z = 2$, $\rho_{calcd} = 1.410$ g cm^{-3}, $\mu = 1.128$ mm^{-1}, $F(000) = 2556$, $2\theta_{max} = 50.0°$. Final residuals (for 265 parameters) were $R1 = 0.0491$ for 2112 reflections with $I > 2\sigma I$, and $R1 = 0.0764$, $wR2 = 0.1577$, GoF = 0.985 for all 3520 data. Residual electron density was 0.753 and -0.574 e Å^{-3}. Highly disordered solvent molecules in the hexagonal channels were modeled as a group of variable-occupancy carbon atoms. CCDC-165791 contains the supplementary crystallographic data for this paper. These data can be obtained free of charge via www.ccdc.cam.ac.uk/conts/retrieving.html (or from the Cambridge Crystallographic Data Centre, 12, Union Road, Cambridge CB21EZ, UK; fax: (+44) 1223-336-033; or deposit@ccdc.cam.ac.uk).
[21] R. W. Jotham, J. A. Marks, S. F. A. Kettle, *Dalton Trans.* **1972**, 428 – 438.
[22] M. Kato, H. B. Jonassen, J. C. Fanning, *Chem. Rev.* **1964**, *64*, 99 – 148.
[23] B. Bleaney, K. D. Bowers, *Proc. R. Soc. London A* **1952**, *214*, 451 – 465.
[24] S. H. Sun, C. B. Murray, D. Weller, L. Folks, A. Moser, *Science* **2000**, *287*, 1989 – 1992.
[25] H. Tamura, K. Shiraishi, H. Takayanagi, *Phys. Status Solidi B* **2001**, *224*, 723 – 725.
[26] X. X. Zhang, S. S. Y. Chui, I. D. Williams, *J. Appl. Phys.* **2000**, *87*, 6007 – 6009.

Substrate Distortion by a β-Mannanase: Snapshots of the Michaelis and Covalent-Intermediate Complexes Suggest a $B_{2,5}$ Conformation for the Transition State

Valérie M.-A. Ducros, David L. Zechel, Garib N. Murshudov, Harry J. Gilbert, Lóránd Szabó, Dominik Stoll, Stephen G. Withers, and Gideon J. Davies*

More than 6000 glycosidase sequences and related open reading frames are currently known. They have been classified into some 85 families based upon amino acid sequence similarities[1] providing a rich context in which to explore variations in glycosidase mechanism. Experimental demonstration of pyranoside ring conformations along the reaction pathway may assist the design of transition state analogues both as therapeutic agents and mechanistic probes. Here we report the three-dimensional structures of the Michaelis complex and covalent glycosyl – enzyme intermediate for a family-26 β-mannanase, both of which display conformational features never previously seen on any glycosidase. When viewed in light of published work on mannosidase inhibition, this work suggests that the transition state for mannoside

[*] Prof. G. J. Davies, Dr. V. M.-A. Ducros, Dr. D. L. Zechel, Dr. G. N. Murshudov
Department of Chemistry
Structural Biology Laboratory
The University of York
Heslington, York, YO10 5DD (UK)
Fax: (+44) 1904-410-519
E-mail: davies@ysbl.york.ac.uk
Prof. H. J. Gilbert, Dr. L. Szabó
Department of Biological and Nutritional Sciences
The University of Newcastle upon Tyne
Newcastle upon Tyne, NE1 7RU (UK)
Dr. D. Stoll, Prof. S. G. Withers
Department of Chemistry
University of British Columbia
2036 Main Mall, Vancouver, BC, V6T 1Z1 (Canada)

Supporting information for this article is available on the WWW under http://www.angewandte.org or from the author.

  1433-7851/02/4115-2824 $ 20.00+.50/0